

## THE IMPACT OF WATER INJECTION-INDUCED FRACTURES ON RESIDUAL OIL DISTRIBUTION IN TIGHT SANDSTONE RESERVOIRS

by

**Xinhua SUN<sup>a,b</sup>, Hailong DANG<sup>a,b</sup>, Mingliang SHI<sup>c\*</sup>,  
Wenqiang LIU<sup>a,b</sup>, Shengsong KANG<sup>a,b</sup>, Qiang WANG<sup>a,b</sup>,  
Yangyang AO<sup>a,b</sup>, and Fengnian ZHAO<sup>a,b</sup>**

<sup>a</sup> Shaanxi Yanchang Petroleum (Group) Limited Liability Company Research Institute, Xi 'an, China

<sup>b</sup> Shaanxi Engineering Research Center of Ultra-Low Permeability Oil and  
Gas Exploration and Development, Xi 'an, China

<sup>c</sup> National Key Laboratory of Petroleum Resources and Prospecting,  
China University of Petroleum (Beijing), Beijing, China

Original scientific paper

<https://doi.org/10.2298/TSCI231005026S>

*This study conducted water-induced fracture experiments and full-diameter core displacement experiments on the cores of a certain oil reservoir in the Ordos Basin, aiming to investigate the impact of these induced fractures of different sizes on displacement efficiency and the distribution of remaining oil, and to perform quantitative analysis. The experimental results indicate that the oil displacement efficiency of the core is related to the depth, angle, and complexity of full-diameter core fractures.*

**Key words:** *tight sandstone reservoirs, water injection-induced fractures, whole core flooding, residual oil distribution, NMR signal*

### Introduction

Due to the influence of deposition and diagenesis, tight sandstone reservoirs exhibit strong heterogeneity, with varying degrees of natural fractures present [1]. In the long-term process of water injection development, improper water injection can lead to the formation of uncontrolled fractures in the injection wells due to the low permeability of the matrix and the high permeability of natural fractures and various artificial fractures, known as injection-induced fractures [2]. The further expansion of these fractures exacerbates the conflict between injection and production in tight oil reservoirs, ultimately resulting in high water cut and severe water flooding in certain directional wells, while the water injection effect in other directional wells is poor [3]. Therefore, a significant amount of research has been conducted to explore the mechanisms of directional water flooding induced between injection and production wells [4].

At the same time, the presence of injection-induced fractures leads to the retention of a significant amount of oil in the reservoir post-water flooding, significantly impacting oil recovery rates [5, 6]. To increase the recovery rate of low permeability reservoirs, researchers both domestically and internationally have conducted numerous displacement experiments and micro-scale simulations to study the distribution characteristics of residual oil [7, 8]. Re-

\* Corresponding author, e-mail: 2021210348@student.cup.edu.cn

search results indicate that when injection pressure exceeds the current minimum horizontal principal stress, and the injection well is aligned parallel to the current maximum horizontal principal stress, fractures only open in the direction of the maximum horizontal principal stress, with residual oil distributed on either side of these fractures. In contrast, when these conditions are not met, fractures open in multiple directions, leading to irregular oil distribution [9, 10].

In summary, previous research has primarily focused on the formation mechanisms of induced fractures and the distribution characteristics of residual oil, with relatively limited research on the impact of induced fractures on the distribution of remaining oil within tight oil reservoirs. Therefore, this study, building on previous research, used full-diameter core preparation for fractures and displacement simulation experimental set-ups to simulate the phenomenon of induced fractures during the water injection development process under reservoir temperature and pressure conditions. Subsequently, through CT scanning and nuclear magnetic resonance, the complexity of fracture morphology and the distribution characteristics of residual oil after fracturing and displacement were quantitatively analyzed. This study provides a theoretical basis for understanding the water flooding patterns in directional wells of tight oil reservoirs.

## **Experimental part**

### *Sample collection and preparation*

The study utilized six tight sandstone core samples from a specific block, collected from three wells. These core samples exhibited varying physical properties and high heterogeneity. Upon receiving these core samples, each sample underwent cleaning and drying procedures, with measured porosities ranging from 12.02% to 13.33% and permeability ranging from 0.040-0.352 mD. These subsurface core samples were processed into cylindrical specimens with a diameter of 100 mm and a length of 150 mm. At the central location on the end face of each core sample, we drilled induction holes with a diameter of 16 mm. Subsequently, induction tubes were inserted into these holes, and epoxy resin was used to seal the cores.

### *Experimental methods and principles*

Conventional core water injection-induced fracture experiments and water flooding experiments are conducted separately. In addition, the confining pressure in the displacement experiments is greater than the displacement pressure, making it impossible for the core to generate fractures. Therefore, in this study, a self-developed integrated fracture and displacement device is employed. It uses a confining pressure system to simulate reservoir conditions, with separate injection ports for inducing and displacing. The inducing port penetrates deep into the core, using a constant injection rate to simulate the actual fracture characteristics in the reservoir. Controlling the scale of injection-induced fractures by altering the depth of the injection wellbore. The results of the water injection-induced fracture experiments are determined based on injection pressure and confining pressure variations. The displacement port is connected to the core holder inlet and uses a constant injection pressure to simulate actual injection characteristics in the reservoir. The dynamic analysis of the core's displacement efficiency is based on the outflow conditions at the outlet.

The main equipment used in the experiment includes a full-diameter core holder, a constant-speed and constant-pressure pump, a pressurization pump, a heating belt, sensors, and more, as shown in fig. 1.

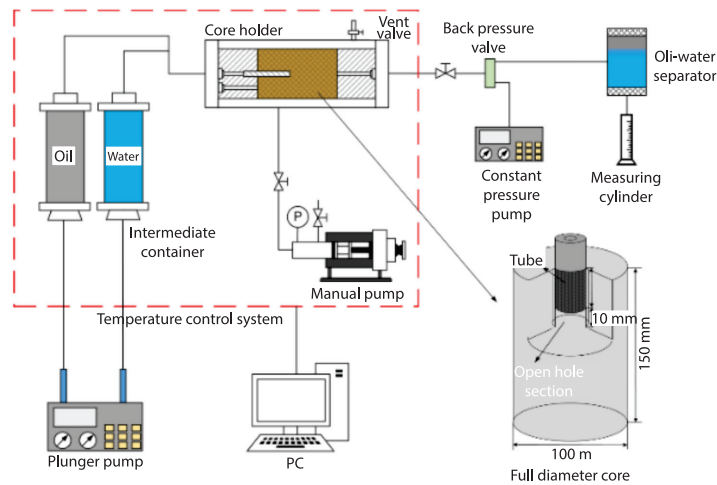


**Figure 1. Schematic of integrated fracturing and displacement experiment with full-diameter core**

## Experimental results and analysis

### *Influence of fractures on oil displacement efficiency*

After conducting CT scans and reconstructions on the six rock cores following the induced crack experiments, the results in fig. 2 reveal that with increasing wellbore depth, the crack dimensions continually enlarge. What were once localized cracks develop into through-cracks, and simple cracks evolve into complex ones. Single cracks branch into multiple fissures, as observed in figs. 2 (b), 2(e), 2(g) or figs. 2(a), 2(c), and 2(f). Furthermore, as the injection volume of the water induction experiment increases, the resulting cracks become longer, and the crack network becomes more complex, as demonstrated in figs. 2(a) and 2(b), 2(c) and 2(e), and 2(f) and 2 (g). Simultaneously, influenced by the subsurface stress, the cracks extend along the direction of maximum principal stress until they penetrate through the wellbore, forming complex penetrating cracks with branches, as seen in figs. 2(e) and 2(g).

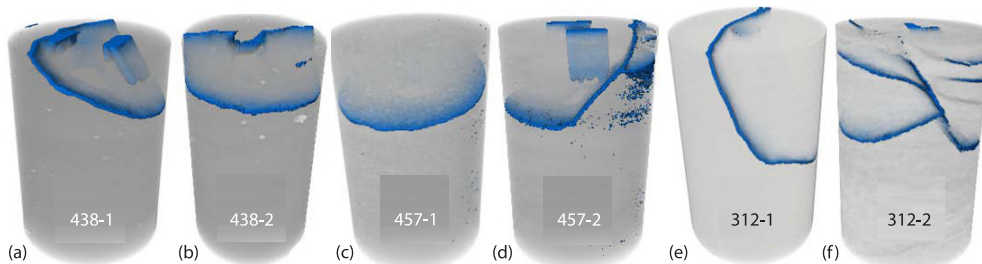


**Figure 2. The 3-D reconstruction of full-diameter rock core water-induced fractures**

Figure 3(a) shows the curve of displacement efficiency of the six core samples as a function of the crack angle. When the angle between the full-diameter core sample's crack and the horizontal direction is small, during the constant pressure displacement process the water pressure acts uniformly on the end face of the full-diameter core sample's crack. This leads to an equal initiation pressure gradient from the crack to the outlet, and the displacement efficiency is essentially unaffected by the crack, as shown in the samples 457-1 and 438-1. However, when

the angle between the full-diameter core sample's crack and the horizontal direction approaches  $90^\circ$ , during the constant pressure displacement process, the water rapidly enters the lower end of the crack, and the water pressure only acts on the part below the crack. This significantly reduces the displacement efficiency, as shown in the samples 312-2 and 438-2. Therefore, the larger the angle between the full-diameter-core-sample's crack and the horizontal direction is, the lower the oil recovery efficiency is.

Figure 3(b) shows the curve of oil recovery efficiency as a function of the crack depth. When the rock has cracks penetrating the top, the displacing water enters the rock along the crack, making it difficult to displace the crude-oil at the crack. Therefore, the deeper the crack, the shorter the path from the end of the crack to the outlet, the less time it takes for the water to be seen during constant pressure displacement, and the lower the rock's oil recovery efficiency, as in the sample 312-2. Figure 3(c) shows the curve of oil recovery efficiency as a function of crack complexity, where the complexity of the crack is represented by fractal dimension. The more complex the crack is, the smaller the area that can flow during the displacement process is, and the lower the oil recovery efficiency is, as in the sample 312-2.

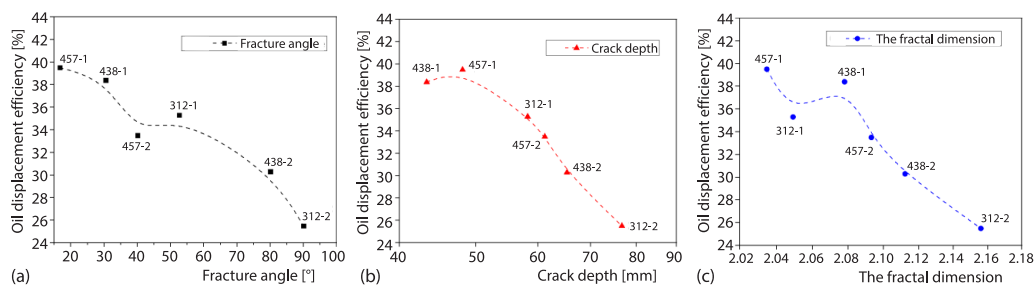


Figure 3. Graphs of oil recovery efficiency as a function of crack angle (a), crack depth (b), and crack complexity (c)

#### Distribution characteristics of residual oil in different pore types

Figure 4 displays the  $T_2$  spectrum distribution curves of the rock samples before and after displacement. The  $T_2$  spectrum distribution curve exhibits a bimodal structure, decreasing from left to right, indicating significant heterogeneity in the pore distribution of the full-diameter core. The left peak has higher signal amplitude, while the right peak has a lower signal amplitude, representing a relatively larger proportion of small pores and a relatively smaller proportion of large pores. In the  $T_2$  distribution plot, the left peak typically corresponds to

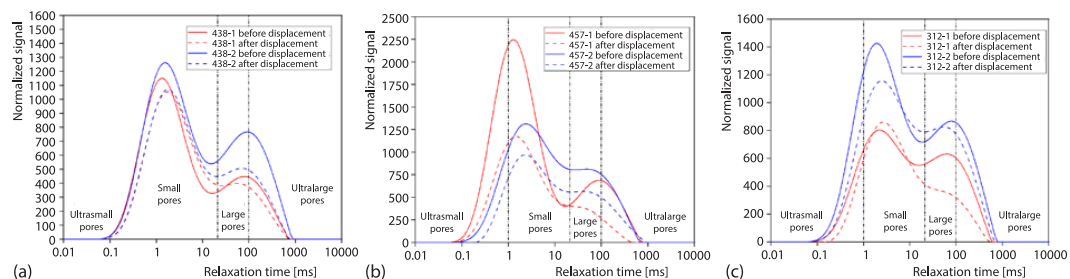


Figure 4. The nuclear magnetic resonance  $T_2$  spectrum distribution curves before and after the displacement of full-diameter rock cores

extremely small pores or clay pores, the middle part corresponds to large and small pores, including bound and free fluid pores, while the right peak corresponds to extremely large pores or fractures.

Based on the amount of signal amplitude reduction in the pores of the six rock samples, it is evident that the larger the fracture size, the greater the reduction in nuclear magnetic resonance signal amplitude. The most significant reductions occur in extremely large and extremely small pores, indicating that the residual oil content in these pores is lower after displacement. Therefore, as fracture size increases, the oil in extremely large and large pores can be more effectively displaced. The fundamental reason for this phenomenon may be that larger fractures result in a larger surface area of contact between the fractures and the displacing water. Under the influence of wettability, the original oil in the rock pores is displaced, allowing the oil to be driven out from the fractures. Therefore, within the same well, both oil displacement efficiency and NMR signal amplitude change rate decrease as fracture size increases. However, there is no clear pattern in the variation between different wells.

#### *Distribution patterns of residual oil in the presence of fractures*

Figure 5 displays 2-D nuclear magnetic resonance (NMR) images generated using spatial phase encoding technology, representing the projection of hydrogen atom imaging on the sagittal plane. The brightness of the images reflects the presence of crude-oil and offers insights into fracture size increases. However, there is no clear pattern in the variation between different wells.

The distribution characteristics of residual oil when compared with the fracture features in CT images. In panels 5(a)-5(e), inclined fractures are present in the rock samples. The upper right part of the rock samples is unaffected by the pressure differential, resulting in the retention of crude-oil and higher brightness. In panels 5(b)-5(c), the rock samples exhibit horizontally penetrating fractures, with displacing water acting uniformly on the fracture surfaces, resulting in the even displacement of crude-oil within the rock samples, with residual oil distributed on both sides of the fractures. In panels 5(d)-5(f), complex fracture network structures are observed, where displacing water only affects the lower portion of the fractures, leaving most of the upper portion's crude-oil undisturbed, resulting in irregular distribution of residual oil.

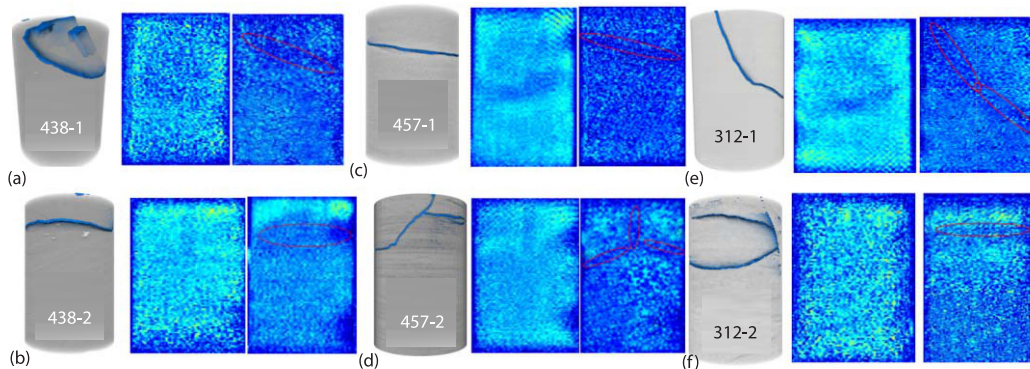


**Figure 5. Rock sample fracture characteristics and residual oil distribution patterns**

By comparing the 2-D NMR and CT imaging, it is evident that in the presence of a single horizontal fracture, residual oil is distributed on both sides of the fracture. In the case of a single inclined fracture, residual oil tends to concentrate in the deeper part of the fracture,

while the shallower region has less residual oil. In the presence of a complex fracture network, the distribution of residual oil becomes irregular.

### Conclusions

This study explored the impact of fractures on oil displacement efficiency through experiments and analyzed the distribution characteristics of residual oil in pores of different scales. The following conclusions and insights were drawn from the experiments:

- The oil displacement efficiency in displacement experiments is related to the depth, angle, and complexity of induced fractures.
- Deeper fractures, larger angles with the horizontal direction, and more complex fractures result in lower oil displacement efficiency in displacement experiments.

Residual oil is primarily distributed in small and extremely small pores, followed by large pores, while almost no residual oil is found in extremely large pores. Larger fracture sizes lead to a more concentrated distribution of residual oil in small pores. Residual oil is distributed on both sides of the fractures, with a concentration of residual oil in the deeper regions of the fractures. In the shallower areas of the fractures, there is less residual oil. When a complex fracture network is present, the distribution of residual oil becomes irregular.

### Acknowledgment

The authors would like to express their gratitude to the Innovation Capability Support of Shaanxi (Program No. 2023-CX-TD-31) and the Technical Innovation Team for Low Carbon Environmental Protection and Enhanced Oil Recovery in Unconventional Reservoirs for their valuable support.

### References

- [1] Zhao, X., *et al.*, Brittleness Characteristics and Its Control On Natural Fractures in Tight Reservoirs: A Case Study from Chang 7 Tight Reservoir in Longdong Area of the Ordos Basin (in Chinese), *Oil and Gas Geology*, 37 (2016), 2, pp. 62-71
- [2] Hustedt, B., *et al.*, Induced Fracturing in Reservoir Simulations: Application of A New Coupled Simulator to a Water Flooding Field Example, *SPE Reservoir Evaluation and Engineering*, 11 (2008), 3, pp. 569-576
- [3] Zhao, X., *et al.*, Characteristics of Waterflood Induced Fracture in Low-Permeability Sandstone Reservoirs and Its Identification Methods: A Case Study from Chang 6 Reservoir in W Area in Ansaioilfield, Ordos Basin (in Chinese), *Oil and Gas Geology*, 38 (2017), 6, pp. 1187-1197
- [4] Liu, H. T., *et al.*, Influence of Fractures on Injection For Low-Permeability Sandstone Reservoir in Taizhao Area, Daqing Oilfield, *Journal of the University of Petroleum*, 29 (2005), 2, pp. 74-78
- [5] Yujia F., *et al.*, Study on Distribution Characteristics of Microscopic Residual Oil in Lowpermeability Reservoirs, *Journal of Dispersion Science and Technology*, 41 (2020), 2, pp. 575-584
- [6] Wang X., *et al.*, Study on Residual Oil Distribution Patterns in Heterogeneous Microscopic Models for Displacement (in Chinese), *Petroleum Geology and Engineering*, 87-90 (2018), 2, pp. 24-125
- [7] Qiu, M., *et al.*, *Study on Micro Occurrence State Description Method of Remaining Oil Based on CTD* (in Chinese), China University of Petroleum (East China), Qingdao, China, 2013
- [8] Fan, F., *et al.*, Study on Quantitative Description Method of Micro Remaining Oil Occurrence State of Reservoir in High Water Cut Stage (in Chinese), *Inner Mongolia Petrochemical Industry*, 1 (2015), 2, pp. 44-46
- [9] Sun, W., *et al.*, Visual Study of Water Injection in Low Permeable Sandstone, *Journal of Canadian Petroleum Technology*, 45 (2006), 2, pp. 21-26
- [10] Saif, T., *et al.*, Microstructural Imaging and Characterization of Oil Shale before and After Pyrolysis, *Fuel*, 197 (2017), June, pp. 562-574